23rd ABCM International Congress of Mechanical Engineering
December 6-11, 2015, Rio de Janeiro, RJ, Brazil

DESIGN AND VALIDATION OF AN AERODYNAMIC BALANCE FOR INMETRO'S WIND TUNNEL

Pollyana de Lima Massari
Pontifical Catholic University of Rio de Janeiro – PUC-RJ
R. Marquês de São Vicente, 225 – Gávea, Rio de Janeiro - RJ
pollyana.massari@gmail.com

Fábio Ouverney Costa
National Institute of Metrology, Quality and Technology (INMETRO)
Fluid Dynamics Metrology Division – Scientific Metrology, Rio de Janeiro – RJ, Brasil
focosta@inmetro.gov.br

Maria Helena Farias
National Institute of Metrology, Quality and Technology (INMETRO)
Fluid Dynamics Metrology Division – Scientific Metrology, Rio de Janeiro – RJ, Brasil
mhfarias@inmetro.gov.br

Abstract. *The aviation, automobile and civil industries are increasingly dependent on new tools to know and improve the performance of their projects, since aerodynamic effects can substantially modify the behavior of a model. When an object is immersed in a fluid flow, it's subjected to moments and forces, which are commonly resolved into two components: the drag and lift forces. To analyze these loads it's essential to have a wind tunnel equipped with an aerodynamic balance, which illustrates these efforts in a quantitative way.*
The aim of this work was to develop and validate an aerodynamic balance, designed and built specifically for the aerodynamic wind tunnel of the Fluid Dynamics Metrology Division from the Brazilian National Institute of Metrology – Inmetro. It was designed using load cells, signal conditioning circuits and a LabVIEW software for data acquisition and processing.
To validate the balance, a NACA 2412 wing profile was used. Tests were done for many angles of attack in different speeds, and the lift and drag coefficients were calculated and compared with literary values. The balance proved to be efficient and coherent when subjected to the application of aerodynamic forces. The results showed good concordance with the literature, for most angles of attack.

Keywords: *aerodynamic balance, drag force, lift force*

1. INTRODUCTION

A model, when immersed in a fluid flow, is subjected to forces and moments (White, 2011). The main loads acting in such model are the drag force, which acts in a direction parallel to the free stream, and lift, which acts in the perpendicular direction. Aerodynamic is the area that studies the role of these forces on models immersed in a fluid. Nowadays, with advances in this field, are remarkable the progresses in aircraft projects, automotive and civil industries, among others. For example, in an aircraft, the wings are designed for the air flow at the bottom to be lower, resulting in a pressure difference, raising a lift force that keeps the aircraft in the air. The aerodynamic effects can substantially modify the aircraft's performance; therefore these concepts are in constant evolution. To analyze all the stresses exerted on models immersed in fluids is of fundamental importance to have an aerodynamic balance, which by means of data acquisition and interpretation illustrates these efforts in a quantitative way.

2. LITERATURE REVIEW

The idea of measuring dynamic forces with a balance is not new. Elftman (1939) has built a platform for measuring the vertical and horizontal forces of the human walking. In their balance there was a base fixed by springs, which suffered a displacement in a point near to the model under study, which was measured, allowing the calculation of the forces. There is still much research to improve and develop new mechanisms, but among the most common balances, there are: balances based in load cells; Sting balances; balances based on mechanical deformation of springs and balances based on Cantilever beam.

In order to prove the safety, determine and improve parameters such as endurance and payload, tests in wind tunnels, including aerodynamics profile, performance, stability and loads are essential, according Suhariyono *et al*.

(2005), which developed a balance consisting of 4 components to study a small aircraft, designed for military surveillance missions.

The balances based on Cantilever beam have one crimped end and another one that is maintained free, where the body to be studied is fixed (Ribeiro, 2010). The displacements in the free end are associated with the drag and lift forces caused by a fluid flow over the tested body. Balances based on mechanical deformation of springs have a relatively simple principle of operation. The model in study is fixed to the balance through rods connected to springs. When the model is subjected to a flow, there is a trend of movement, causing a displacement of those springs which are initially set to a zero load situation, i.e. the deformation when the model is at rest. The forces are calculated analyzing the displacement of the springs, made according to the applied load (Ribeiro, 2010). In most balances, it's necessary to use supports, such as springs or metal rods, which may cause interference in the study; therefore, there are balances that are designed with magnetic suspension systems. Lee *et al*. (2013) used this technique, engaging magnets in a NACA profile in study.

3. BASIC PRINCIPLES

3.1 Drag and Lift Forces

The drag force is the component that acts as a resistance force when a body is moving in a fluid. It has the same direction and sense of the flow. This force tends to increase as the body's velocity increase. In the case of the aircraft industry the designs are tested by varying the geometry of the profiles in order to minimize the drag, thus improving performance. The drag coefficient (C_d) is a dimensionless number used to quantify the resistance of a body in a fluid flow, which is related to the drag force by the equation:

$$F_d = C_d \frac{\rho V^2 A}{2} \tag{1}$$

Where C_d is the drag coefficient, ρ is the fluid density (kg/m³), V is the velocity (m/s) and A is the area (m^2).

The lift force is the aerodynamic component that is perpendicular to the flow direction, and is primarily responsible for supporting the weight of a plane. The lift coefficient is a function of the profile template, the number of Reynolds and angle of attack. The lift force (F_l) is given by the equation:

$$F_l = C_l \frac{\rho V^2 A}{2} \tag{2}$$

Where C_l is the lift coefficient, ρ is the fluid density (kg/m³), V is the velocity (m/s) and A is the area (m^2).

3.2 Inmetro's Aerodynamic Wind Tunnel

One of the most important facilities in aerodynamics research is the wind tunnel, which reproduces an air flow in a controlled and repetitive way, which will interact with a model in the test section. The information collected in the tests are used to improve the design of a body affected by a flow. An aerodynamic balance, coupled to this facility, is able to determine the loads and aerodynamic interactions that the fluid exerts on the model, and to verify if the design requirements have been achieved. The aerodynamic wind tunnel of the Fluid Dynamics Metrology Division from the Brazilian National Institute of Metrology – Inmetro - was made of wood structure, with metal frames and polycarbonate windows for visualization, as shown in Fig. 1. The internal test section has a square cross area, with 0.5 m of side. The tunnel has total length of 8 m and the maximum speed is 23 m/s. To determine the flow velocity within the test section, the wind tunnel characterization was made with a calibrated ultrasonic anemometer.

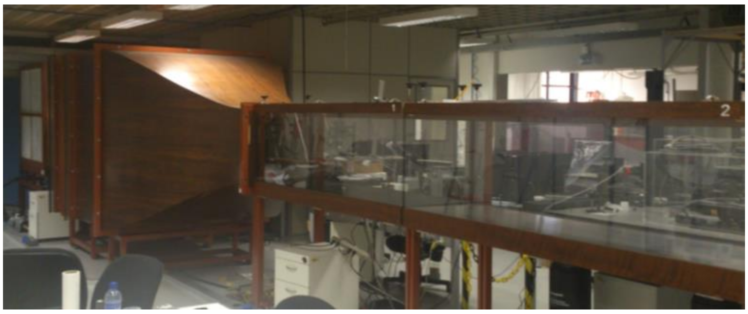

Figure 1. Aerodynamic wind tunnel of Inmetro

4. THE AERODYNAMIC BALANCE DESIGN

4.1 Apparatus for Measurement of the Lift Force

To measure the lift force on the model, load cells were used as the sensing element for the measurements. First, two L-shaped metal profiles were fixed above the wind tunnel, one on each side, to support the balance (Fig. 2), in which metal spheres were coupled to assist in supporting the structure and thus preventing friction in the vertical direction, as shown in Fig. 3.

The balance structure is composed by a metal frame with a device for holding the rods attached to the model and adjusting the angle of attack. Spheres were placed to focus the normal force to a single point in the load cell.

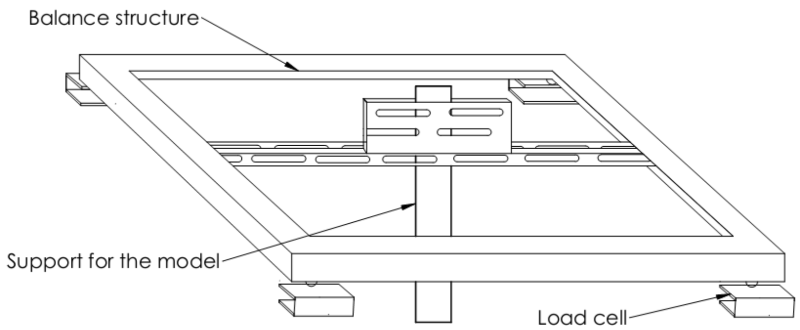

Figure 2. Schematic drawing of the assembly

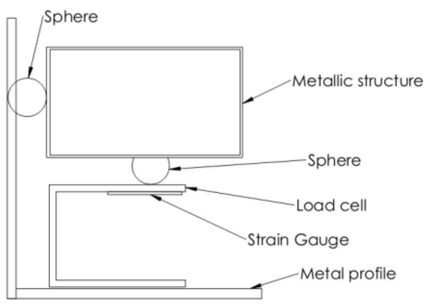

Figure 3. Side view of the assembly

To build the load cell a C-Profile was chosen, since it has a high sensitivity to the load application. The way of bonding the strain gauges is also a very important factor for a good measurement. To determine the most effective position for bonding the sensors, the maximum curvature criteria was used, where the maximum sensitivity in a single direction could be obtained and thus the components of forces could be uncoupled. Considering negligible shifts in the side of the C profile, the top part, in which the strain gauges were installed, can be modeled as a cantilever beam. Therefore, the maximum values of both compression and traction are located close to the crimping of the beam, as shown in Fig. 4. This is the best place for bonding the strain gauge.

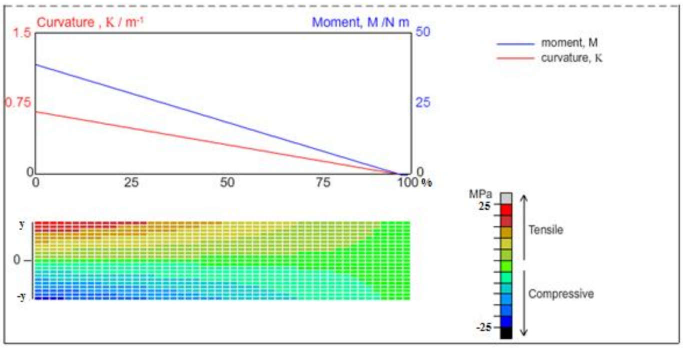

Figure 4. Stresses profile for cantilever beam

4.1.1 Strain Gauge Signal Reading

The extensometer is a widely used method to analyze tensions and deformations that a mechanical structure suffers due to a load or to the effect of temperature. The strain gauge measures the deformation by the variation of an electric resistance. For measuring the deformation (and thus the forces applied to the load cells), it was built one independent transduction circuit for each strain gauge, based on a ¼ Wheatstone bridge circuit, as shown in Fig. 5:

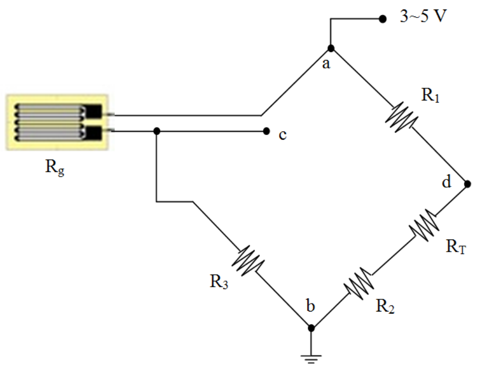

Figure 5. Strain gauge on the Wheatstone bridge

For each circuit, it were used three 120 Ω resistors (R_1 R_2 and R_3), the same resistance of strain gauge (R_g). A 10 Ω potentiometer (R_T) was used in series with R_2 to balance the bridge. The bridge must be powered between the nodes a and b (V_{ab}), with a 4V maximum voltage source. The general equation for the voltage between nodes c and d is given by:

$$\left(\frac{R_g}{R_g + R_3} - \frac{R_1}{(R_2 + R_T) + R_1}\right) V_{ab} = V_{cd} \tag{3}$$

The voltage between nodes c and d (V_{cd}) is zero in a balanced condition. When the load cell is subjected to a deformation, there is a little change in R_g value, unbalancing the bridge and generating a voltage between nodes c and d. Due to the low amplitude of the signal generated by the strain gauges, the signal to noise ratio (SNR) is typically very low. As the measurements will be carried on steady state, the frequency of the interest of the signal must be low and it is possible to improve the signal quality by filtering high frequency components. The most common form to carry out this operation is using a low-pass filter in the electronic circuit. An instrumentation amplifier was also used in order to amplify the filtered signal and suppress common mode noise.

The final circuit for signal conditioning can be observed in Fig 6. The output of each signal was connected to a data acquisition board connected to a computer.

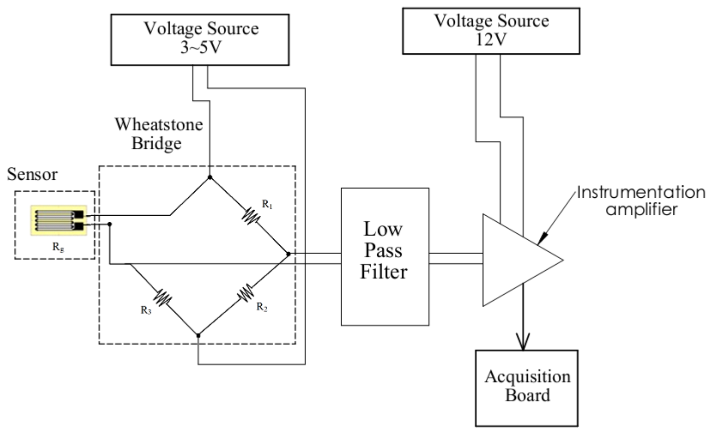

Figure 6. Signal conditioning circuit

For processing the acquired data, a LabVIEW® program was created, where both power voltage and signals were monitored for each circuit.

The developed program is divided into two main parts. At first, the balance is tared. With the balance at rest, the instantaneous values from the strain gauges are read for 5 s, and the mean values for each sensor are stored. In a second step, the readings of the data acquisition board are done continuously and in real time. The values obtained during the first step are used to eliminate any hysteresis error, by subtracting the instantaneous values by the values obtained in the first step. After this operation, the signal is multiplied by a constant of the sensor, which was obtained during the adjustment phase. This constant converts the signals of voltage in to force.

4.1.2 Adjustment of the Load Cells

First, each load cell was separately subjected to the action of the weight of known masses. Thus, it was possible to obtain the proportionality constant of each sensor. After that, with the balance assembled, a number of load applications in the sense contrary to gravity (relieving the preload in the load cell due to the weight of the balance) were applied, in order to detect potential problems and to find a global constant of the balance. The results of this second stage showed that in the actual situation of use, the sensors responded linearly to the actions of vertical forces.

4.1.3 Mathematical Modeling for Determining Lift Force

Initially, the angle of attack of the airfoil is defined and the balance is then reset. In the neutral situation, there is a natural deformation in the load cells due to the weight of the balance. When the fan is turned on, an air stream flows through the airfoil, and a lift force F_l acts decreasing the deformation of the load cells. The lift force is then calculated from the readings of the signals generated by the sensors. Figure 7 shows the forces diagram.

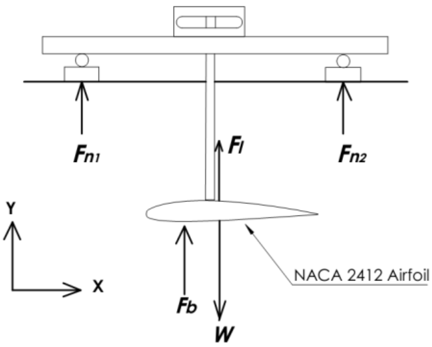

Figure 7. Distribution of forces to calculating the lift force

Where F_b is the buoyancy force, F_n are the normal forces and W is the total weigh. Analyzing the forces system:

$$F_{n_1} + F_{n_2} + F_{n_3} + F_{n_4} - \mathrm{W} + F_l + E = 0 \quad (4)$$

Disregarding the buoyancy force, the lift force will be:

$$F_l = W - F_n \quad (5)$$

4.2 Apparatus for Measurement of the Drag Force

The mechanism created to measure the drag force is a little different than the one created to determine the lift force. For uncoupling the lift force to the drag force, a platform with freedom of movements in the wind tunnel's axial direction, composed of a linear guide and low friction skates, was created. This platform exerts a force in a load cell (similar to the ones used to determine the lift force) with the same intensity of the drag force, as shown in Fig. 8. The signal conditioning system, data acquisition system and data treatment were exactly the same as described in section 4.1.

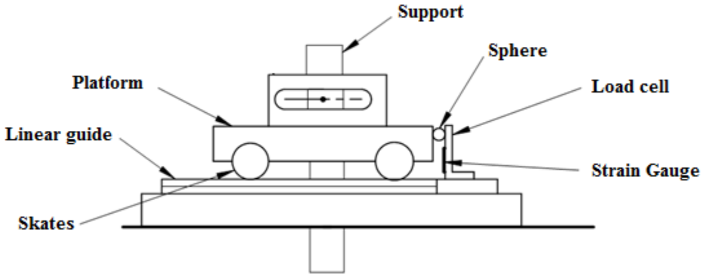

Figure 8. Apparatus for measuring axial forces

4.2.1 Mathematical Modeling for Determining Drag Force

Analogously to the procedure for calculating the lift force, first, it was defined the angle of attack of the airfoil. With the fan off, the mobile platform was positioned very close to the load cell. Thus, when the tunnel is turned on, the sensor will not suffer an impact due to the kinetic energy of the mobile platform. The flow interacts with the model in study, rising a drag force F_d. The forces diagram is shown in Fig. 9.

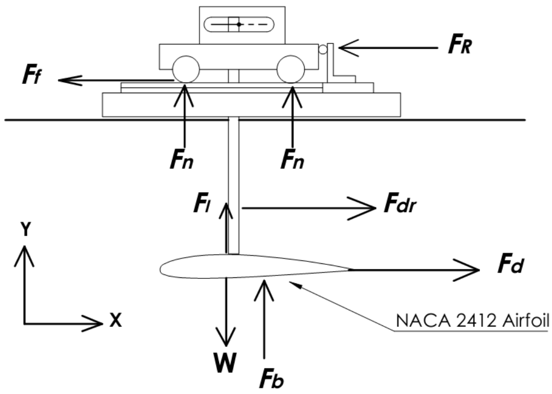

Figure 9. Distribution of forces to calculating the drag force

Analyzing forces system, in the x axis:

$$F_d = \mu F_n + F_R - F_{dr} \tag{6}$$

Where F_n is the normal force, μ is the friction coefficient, F_R is the sensor resultant force and F_{dr} is the rods drag force. Thus:

$$F_d = \mu_e(F_P - F_l) + F_R - F_{ds} \tag{7}$$

Analyzing forces system, in the y axis:

$$F_n + F_l + F_b = W \tag{8}$$

Where F_b is the buoyancy force and W is the total weigh. Both rods drag force F_{ds} and friction coefficient μ were calculated experimentally. Therefore, the drag force will be:

$$F_d = \mu (W - F_l) + F_R - F_{dr} \tag{9}$$

5. VALIDATION OF THE AERODYNAMIC BALANCE

After the system design and assembly, the apparatus validation is extremely important to ensure that it is effective in what it proposes. For this, the results obtained in the experiments shall be compared with those presented in literature or through computer simulations. To validate the balance, a NACA 2412 (UIUC, 2014) profile was used. The most important point to note when positioning a model in a wind tunnel is to satisfy the condition that the fixing method will not affect the flow, minimizing errors and masking results. This question is related to the blocking and wall effects. Therefore, the maximum wingspan of the airfoil must be less than 80% of width of the test section (Pope *et al.*, 1999). Knowing the side of the test section, the chosen NACA profile can be up to 0.40 m, as shown in Fig. 10.

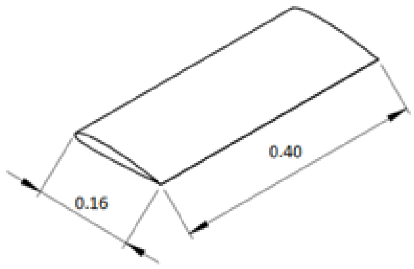

Figure 10. NACA 2412 Profile (dimensions in m)

A results comparison method was chosen. The X-Plane 10® is a flight simulator developed by Laminar Research, considered the most comprehensive and realistic in the world for personal computers. A supplement contains several aircraft wing profiles with their respective drag and lift coefficients values, and it's data was used for comparison.

6. RESULTS AND DISCUSSION

The NACA 2412 profile was tested in up to eleven different velocities, with variations in the angle of attack of 5°, 10°, 13°, 15°, 17.8° and 20°, but not all results will be shown in this paper. For larger angles, the flow velocity was limited due the fragility of the wing model. Therefore, the expected lift force was calculated by Eq. (2), for each angle of attack. Comparing the theoretical results of the lift force with the ones obtained with the balance, the graphics for angle of attack of 10°, 15°, 17.8° and 20° are shown in Fig 11. Looking at the graphs, one can see that the forces obtained for the angles of attack of 13°, 17.8° and 20° exhibit good regularity with the expected values. For the smaller angles of 5° and 10° only for low speeds the balance responded coherently. As expected, the lift coefficient values obtained in experiment to angle of attack of 5° and 10°, growth tendency proportional to the square of speed, but with some lag. For these smaller angles, the force is expected to be very small, causing the relative error to be larger. Results for angles of attack of 13° 17.8° and 20° were more consistent. Conversely, the result for the angle of 15° showed disagreement with the theory. It may be associated with an unstable situation, possibly caused by a resonance effect.

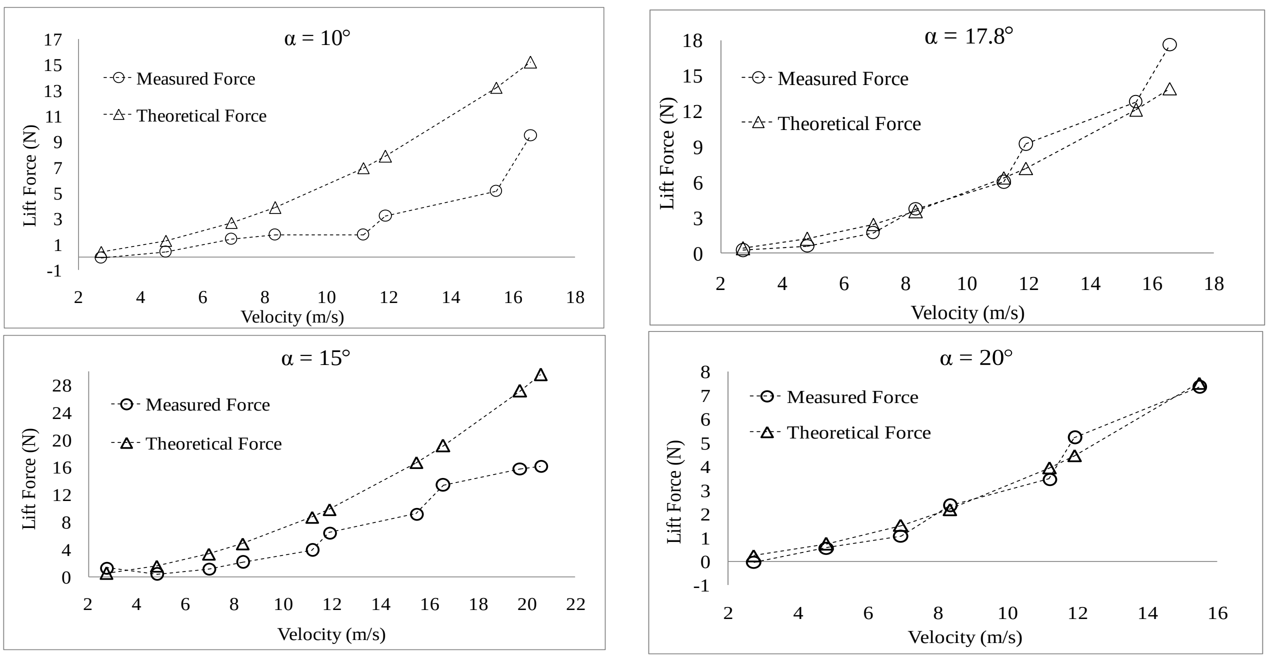

Figure 11. Results for lift force

The NACA 2412 profile was also tested to the drag force in up to eleven different speeds, with variations in the angle of attack of 0°, 5.4°, 10°, 15° and 19°. Using the Eq. (1) and knowing the *Cd* values, one can obtain the expected theoretical force for each angle of attack. Comparing these results with the ones obtained by the balance, graphs of Fig. 12 were plotted for the angles of attack of 5.4° and 10°.

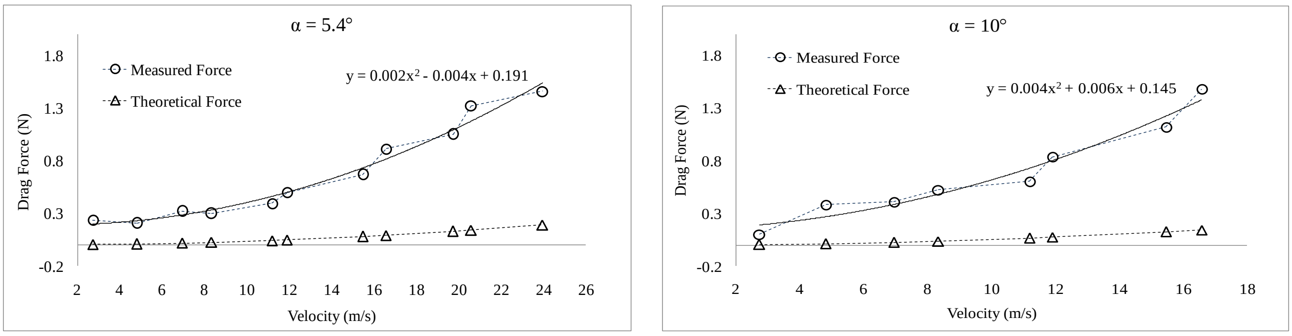

Figure 12. Results for drag force

Despite the differences in the measured values compared to the theoretical values, results obtained experimentally in aerodynamic wind tunnel showed satisfactory results, since the drag force has a growth tendency proportional to the square of speed. It was expected in advance that the measured drag coefficient values did not presented a good agreement with the theory, due to the large amount of influential factors. The total drag force acting on an airfoil has a large contribution of viscous shear drag and pressure drag, making it more complex to measure this force without calculating these components separately. Two other effects that became extremely influential in these calculations were the edge effect and the hysteresis.

7. CONCLUSION

In this work, the main objective has been achieved, the design and assemble of an aerodynamic balance to quantify flow efforts, developed specifically for Inmetro's aerodynamic wind tunnel. Even if dealing with a simplified construction, the balance proved to be efficient and responded coherently when subject to the application of aerodynamic forces.

The tests performed with the balance, provided results for lift and drag forces as a function of the angular variation for the NACA 2412 profile. Although some values presented difference between the studies obtained in literature, the results showed good compatibility for most of the tested angles.

8. REFERENCES

Ismail, R. A. K., 2003. *Balança Aerodinâmica de Quatro Componentes*. Faculdade de Engenharia Mecânica – UNICAMP, São Paulo.

Elftman H., 1939. *Forces and energy changes in the leg during walking*. American Journal of Physiology, Columbia University, New York City.

Lee, K. D. *et al*., 2013. *Dynamic calibration of magnetic suspension and balance system for sting-free measurement in wind tunnel tests*. Journal of Machanical Science and Technology.

Pope, A.; Rae, W. H.; Barlow, J., 1999. *Low speed Wind Tunnel Testing.* John Wiley & Sons, 3º edition, USA.

Ribeiro, A. F. et al., 2010. *Balança Aerodinâmica de Princípio Eletromecânico para Instrumentação em Túnel de Vento*. Congresso Nacional de engenharia Mecânica – CONEM 2010, Campina Grande, PB, Brasil.

UIUC Applied Aerodynamics Group, 2015. Departament of Aerospace Engennering. 02 Set. 2014. <http://m-selig.ae.illinois.edu/ads/afplots/naca2412.gif>. Acesso: 02 set. 2014.

Suhariyono, A. *et al*., 2005. *Design of precision balance and aerodynamic characteristic measurement system for micro aerial vehicles*. Sience Direct, South Korea.

White, F. M., 2011. *Fluid Mechanics* McGraw-Hill, New York, 7th edition.

9. RESPONSIBILITY NOTICE

The authors are the only responsible for the printed material included in this paper.